Supporting Information

Layer number identification of intrinsic and defective multilayer graphenes up to 100 layers by the Raman mode intensity from substrate

Xiao-Li Li[1], Xiao-Fen Qiao[1], Wen-Peng Han[1], Yan Lu[1], Qing-Hai Tan[1], Xue-Lu Liu[1], and Ping-Heng Tan[1]

1.State Key Laboratory of Superlattices and Microstructures, Institute of Semiconductors, Chinese Academy of Sciences, Beijing 100083, China. E-mail: phtan@semi.ac.cn

Raman intensity in multilayer structure is determined by multiple reflection at the interfaces and optical interference within the medium. We adopted the multiple reflection interference method[1–4] to calculate the Raman mode intensity of a medium in the multilayer structure. When NLG flakes are deposited on SiO_2/Si substrate, the four-layer structure can be established, containing air($\tilde{n}_0$), NLG($\tilde{n}_1$, d_1), SiO_2($\tilde{n}_2$, d_2), Si($\tilde{n}_3$, d_3), where $\tilde{n}_i$ and d_i (i=0,1,2,3) are the complex refractive index and the thickness of each medium, as demonstrated in Fig. S1.

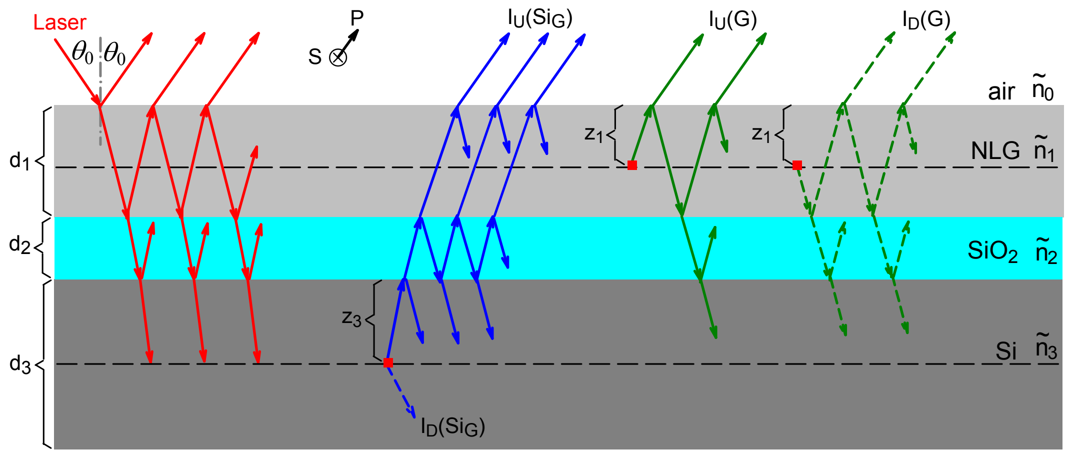

Figure S1: Schematic diagrams of multiple reflection and optical interference in the multilayer structures containing air, NLG, SiO_2, and Si for the incident laser and out-going Raman signals (the G peak from NLG and the Si peak from Si substrate). $\tilde{n}_0$, $\tilde{n}_1$ (d_1), $\tilde{n}_2$(d_2), and $\tilde{n}_3$(d_3) are the complex refractive indices (thickness) of air, NLG, SiO_2 and Si layers, respectively.

In the following text, we will discuss how to calculate the Raman intensities of I(Si_0), I(Si_G) and I(G), where I(Si_0) is the Raman intensity of the Si mode from SiO_2/Si substrate which is not covered by NLG flakes, I(Si_G) is the Raman intensity of the Si mode from SiO_2/Si substrate underneath NLG flakes, and I(G) is the Raman intensity of the G mode from NLG flakes deposited on SiO_2/Si substrate.

Similar to previous works[1–4], to calculate the intensity of Raman signal from the multilayer structures, one must treat the laser excitation and Raman scattering processes separately. The laser intensity profile does not decrease monotonically toward the Si layer due to multiple reflection and optical interference in the multilayer structures. So, Raman signals from the depth z_1 in the NLG flake and from the depth z_3 in the Si layer will be excited by the laser excitation power at the corresponding depth. The multiple reflection and optical interference are also taken into account in the transition process of Raman signal from the active layers to air. We defined F_L and F_R as respective enhancement factors for laser excitation and Raman signal, similar to the notation of Yoon *et al.*[2,4]. The Raman intensity of a given phonon mode from the medium i can be expressed by integrating over its thickness, d_i, as following equation:

$$I \propto \int_0^{d_i} |F_L(z_i)F_R(z_i)|^2 dz_i. \tag{1}$$

The transfer matrix formalism can be used to calculate F_L and F_R in the multilayer structures, which has been widely used to calculate the Raman signal and optical contrast of NLG flakes on SiO_2/Si substrate.[3,5,6] In order to take the numerical aperture NA of the objective into account, we calculate contributions from each portion of the laser beam by integrating the incident angle θ from 0 to $\arcsin(NA)$. The s-polarization (transverse electric field, $\vec{E}$, perpendicular to the graphene c-axis) and p-polarization (transverse magnetic field, $\vec{H}$, associated to electric field by $\vec{H} = \tilde{n}\vec{E}$) field components[5] are also treated for the transfer matrices. The beam expander is adopted in the optical path to make that the laser beam can be regarded as an ideal parallel beam so that the Gaussian intensity distribution of the incident laser beam is ignored in the calculation. Given that the different polarization dependence of the Raman modes of NLG and substrates due to their different lattice symmetry, the Raman tensor **R** of each phonon mode is also considered. Thus, the total Raman intensity of a Raman mode from the dielectric multilayer is given by integrating over the solid angle (θ, φ for the laser beam and θ', φ' for the Raman signal) of microscope objective with a numerical aperture of NA and the depth (z_i) in the dielectric layer i:

$$I \propto \int_0^{d_i} \int_0^{\theta'_{max}} \int_0^{2\pi} \int_0^{\theta_{max}} \int_0^{2\pi} \sum_{i=s,p_\perp,p_\parallel} \sum_{j=s',p'_\perp,p'_\parallel} \left| F_L^i(z_i,\theta,\varphi)(\overrightarrow{e}_R^j \cdot \mathbf{R} \cdot \overrightarrow{e}_L^i) F_R^j(z_i,\theta',\varphi') \right|^2 \sin\theta\cos\theta d\theta d\varphi \sin\theta' \cos\theta' d\theta' d\varphi' dz_i, \tag{2}$$

where $\overrightarrow{e}_R$ and $\overrightarrow{e}_L$ are the electric field vectors of the Raman signal and laser excitation at the depth z_i, respectively.

We use the transfer matrix formalism calculate F_L and F_R in Eq. (2). The transmission and reflection of total electric and magnetic fields in the four-layer structure can be described by characteristic matrices A_{ij} and $B(z_j)$, where A_{ij} describes the propagation across the interface from i to j layer applying the boundary conditions, and $B(z_j)$ denotes the propagation through the j layer at depth z_j.

The s-polarization and p-polarization field components are treated separately in analyzing the characteristic matrices. $A_{ij}^{s(p)}$ can be expressed as follows:

$$A_{ij}^{s(p)} = \frac{1}{t_{ij}^{s(p)}} \begin{pmatrix} 1 & r_{ij}^{s(p)} \\ r_{ij}^{s(p)} & 1 \end{pmatrix} \tag{3}$$

where $t_{ij}^{s(p)}$ and $r_{ij}^{s(p)}$ are transmission and reflection coefficients from i to j layer for s-polarization and p-polarization, which depend on the complex refractive index $\tilde{n}_i, \tilde{n}_j$ and the refracted angle θ_i, θ_j. The complex refractive index in the dielectric layer i is denoted by $\tilde{n}_i(\lambda) = n_i(\lambda) - ik_i(\lambda)$, which is dependent on λ. Similar to previous works, we consider only the in-plane complex refractive index of graphene, and thus the s- and p-components of laser excitation can share the same expression. In fact, the contribution from the out-of-plane complex refractive index of graphene can be ignored because the out-of-plane n_1 of graphene is far smaller than the in-plane one and the out-of-plane k_1 is almost zero[7]. The refracted angle θ_i in the dielectric layer i is calculated with the Snell law. The $t_{ij}^{s(p)}$ and $r_{ij}^{s(p)}$ are expressed as: $t_{ij}^s = \frac{2\tilde{n}_i\cos\theta_i}{\tilde{n}_i\cos\theta_i + \tilde{n}_j\cos\theta_j}$, $r_{ij}^s = \frac{\tilde{n}_i\cos\theta_i - \tilde{n}_j\cos\theta_j}{\tilde{n}_i\cos\theta_i + \tilde{n}_j\cos\theta_j}$, $t_{ij}^p = \frac{2\tilde{n}_i\cos\theta_i}{\tilde{n}_j\cos\theta_i + \tilde{n}_i\cos\theta_j}$, $r_{ij}^p = \frac{\tilde{n}_j\cos\theta_i - \tilde{n}_i\cos\theta_j}{\tilde{n}_j\cos\theta_i + \tilde{n}_i\cos\theta_j}$.

$B(z_j)$ can be expressed as follows:

$$B(z_j) = \begin{pmatrix} e^{i\delta(z_j)} & 0 \\ 0 & e^{-i\delta(z_j)} \end{pmatrix} \tag{4}$$

where $\delta(z_j) = 2\pi\tilde{n}_j z_j \cos\theta_j/\lambda$ is phase factor, which is determined by the propagation distance z_j of laser or Raman scattering lights in j layer. The differences between the wavelengths of the laser and Raman signal of the G peak or Si peak should be considered in $t_{ij}^{s(p)}$, $r_{ij}^{s(p)}$ and $\delta(z_j)$ due to the λ-dependent complex refractive index for each layer.

The complete transfer matrix for the whole multilayer structures can be obtained by multiplication of above simple matrices.

1. Raman intensity of the G mode, I(G)

Schematic diagrams of the laser excitation and Raman scattering processes for the G mode are given in Fig. S1. For the Raman signal from the depth z_1 in NLG flakes, we will first calculate the electric field components of the laser at z_1 and then calculate the collected G intensity in air that excited at z_1 by the laser excitation.

The relation between electric field components of laser in air, E_{L0}, and at the depth z_1 in NLG, E_{LG}, can be expressed by a transfer equation of

$$\begin{pmatrix} E_{L0}^{s(p),+} \\ E_{L0}^{s(p),-} \end{pmatrix} = A_{01}^{s(p)} B(z_1) \begin{pmatrix} E_{LG}^{s(p),+}(z_1) \\ E_{LG}^{s(p),-}(z_1) \end{pmatrix} \tag{5}$$

where the symbols $+,-$ denote light propagating directions from air to the dielectric layers and the opposite direction. $E_{L0}^{s(p),+}$ is the electric field component of laser source in air, which is assumed as 1. $E_{LG}^{s(p),+}(z_1)$ and $E_{LG}^{s(p),-}(z_1)$ are the electric field components with $+,-$ directions arriving at the depth z_1 in NLG. The laser excitation enhancement factors can be calculated by $F_L^s(z_1) = E_{LG}^{s,+}(z_1) + E_{LG}^{s,-}(z_1)$, $F_L^{p\perp}(z_1) = (E_{LG}^{p,+}(z_1) - E_{LG}^{p,-}(z_1))\cos\theta_1$ and $F_L^{p\|}(z_1) = (E_{LG}^{p,+}(z_1) + E_{LG}^{p,-}(z_1))\sin\theta_1$.

To obtain electric field components at the depth z_1 in NLG, $E_{LG}^{s(p),+(-)}(z_1)$, the corresponding boundary conditions related with Si layer must be considered. Thus, the transfer equation of laser excitation in the whole four-layer structure must be taken into account. Because laser excitation passes through interfaces of air/NLG, NLG/SiO_2 and SiO_2/Si, and finally absorbed by the Si layer, the transfer equation is expressed as

$$\begin{pmatrix} E_{L0}^{s(p),+} \\ E_{L0}^{s(p),-} \end{pmatrix} = A_{01}^{s(p)} B(d_1) A_{12}^{s(p)} B(d_2) A_{23}^{s(p)} \begin{pmatrix} E_{LS}^{s(p),+}(0) \\ 0 \end{pmatrix} \tag{6}$$

where $E_{LS}^{s(p),+}(0)$ is the incident electric field component into the Si layer. $E_{L0}^{s(p),-}$ can be figured out by Eq. (6). Substituting it into Eq. (5), $E_{LG}^{s(p),+(-)}(z_1)$ can be calculated and $F_L^{s(p\perp,p\|)}(z_1)$ can be obtained.

The Raman scattering process is more complicated than the laser excitation process. Because the emission direction of photons for Raman signal is full of all the solid angles, one must consider two pathways for the emission of Raman signal[3]: toward (up,U) and away from (down,D) the NLG surface close to air, as illustrated in Fig. S1, and the corresponding Raman intensities are denoted as $I_U(G)$ and $I_D(G)$. Similarly, the two Raman transfer process from the depth z_1 in the NLG to air can be expressed by transfer equations as follows:

$$\begin{pmatrix} 0 \\ E_{R_{U0}}^{s'(p'),-} \end{pmatrix} = A_{01}^{s'(p')} \left[B(d_1) \begin{pmatrix} E_{R_{UG}}^{s'(p'),+}(d_1) \\ E_{R_{UG}}^{s'(p'),-}(d_1) \end{pmatrix} + B(z_1) \begin{pmatrix} 0 \\ E_{R_{UG}}^{s'(p'),-}(z_1) \end{pmatrix} \right] \tag{7}$$

and

$$\begin{pmatrix} 0 \\ E_{R_{D0}}^{s'(p'),-} \end{pmatrix} = A_{01}^{s'(p')} \left[B(d_1) \begin{pmatrix} E_{R_{DG}}^{s'(p'),+}(d_1) \\ E_{R_{DG}}^{s'(p'),-}(d_1) \end{pmatrix} - B(z_1) \begin{pmatrix} E_{R_{DG}}^{s'(p'),+}(z_1) \\ 0 \end{pmatrix} \right] \tag{8}$$

where $E_{R_{U0}}^{s'(p'),-}$ and $E_{R_{D0}}^{s'(p'),-}$ are the electric field components of Raman signal related with 'U' and 'D' pathways in air, $E_{R_{UG}}^{s'(p'),-}(z_1)$ and $E_{R_{DG}}^{s'(p'),+}(z_1)$ are the electric field components of Raman signal sources related with 'U' and 'D' pathways at the depth z_1 in the NLG, respectively. The s and p components of Raman scattering light is marked as s' and p' ones to distinguish them from the laser excitation. We assume $E_{R_{UG}}^{s'(p'),-}(z_1) = E_{R_{DG}}^{s'(p'),+}(z_1) = 1$, and thus the Raman scattering enhancement factors can be calculated by $F_R^{s'}(z_1) = E_{R_{U0}}^{s',-} + E_{R_{D0}}^{s',-}$, $F_R^{p'_\perp}(z_1) = (E_{R_{U0}}^{p',-} - E_{R_{D0}}^{p',-})\cos\theta'_1$ and $F_R^{p'_\parallel}(z_1) = (E_{R_{U0}}^{p',-} + E_{R_{D0}}^{p',-})\sin\theta'_1$.

To obtain electric field components $E_{R_{U0}}^{s'(p'),-}$ and $E_{R_{D0}}^{s'(p'),-}$, the corresponding boundary conditions related with Si layer must be considered. Because the Raman signal from NLG flakes also passes through are/NLG, NLG/SiO_2 and SiO_2/Si interfaces, and is absorbed finally by the Si layer, the corresponding transfer equation is expressed as follows:

$$\begin{pmatrix} E_{R_{UG(DG)}}^{s'(p'),+}(d_1) \\ E_{R_{UG(DG)}}^{s'(p'),-}(d_1) \end{pmatrix} = A_{12}^{s'(p')} B(d_2) A_{23}^{s'(p')} \begin{pmatrix} E_{R_{US(DS)}}^{s'(p'),+}(0) \\ 0 \end{pmatrix} \tag{9}$$

where $E_{R_{US(DS)}}^{s'(p'),+}(0)$ is the electric field component of the G mode transmitted into the Si layer.

With the transfer equation Eq. (9), the ratio of $E_{R_{UG}}^{s'(p'),-}(d_1)$ to $E_{R_{UG}}^{s'(p'),+}(d_1)$ and the ratio of $E_{R_{DG}}^{s'(p'),-}(d_1)$ to $E_{R_{DG}}^{s'(p'),+}(d_1)$ can be calculated. Finally, $E_{R_{U0(D0)}}^{s'(p'),-}$ and $F_R^{s'(p'_\perp,p'_\parallel)}(z_1)$ can be obtained based on the transfer equations Eq. (7)-(9).

The total Raman intensity of the G mode can be calculated by the formula Eqs. (2), when the Raman tensor **R** of the G peak for graphene is considered.

2. Raman intensity of the Si mode, I(Si_G)

For the calculation of I(Si_G), the laser arrives at the Si layer and is absorbed finally. Thus, no laser components at any depths in the Si layer are transmitted back toward the interface between Si and SiO_2. The transfer equation for the laser transmission from air to the depth z_3 in the Si layer is expressed as follows:

$$\begin{pmatrix} E_{L0}^{s(p),+} \\ E_{L0}^{s(p),-} \end{pmatrix} = A_{01}^{s(p)} B(d_1) A_{12}^{s(p)} B(d_2) A_{23}^{s(p)} B(z_3) \begin{pmatrix} E_{LS}^{s(p),+}(z_3) \\ 0 \end{pmatrix} \tag{10}$$

The laser excitation enhancement factors in this process can be calculated by $F_L^s(z_3) = E_{LS}^{s,+}(z_3)$, $F_L^{p\perp}(z_3) = E_{LS}^{p,+}(z_3)\cos\theta_3$ and $F_L^{p\|}(z_3) = E_{LS}^{p,+}(z_3)\sin\theta_3$. $E_{LS}^{s(p),+}(z_3)$ can be calculated only with the transfer equation Eq. (10) and $F_L^{s(p\perp,p\|)}(z_3)$ can be obtained.

For the Raman scattering process of the Si mode, only one pathway for the emission of Raman signal toward (up,U) the interface between Si and SiO_2 is considered, and that away from (down,D) the interface between Si and SiO_2 is absorbed by the Si layer, as illustrated in Fig. S1, and the corresponding Raman intensity is denoted as $I_U(Si_G)$. The transfer equation for the Raman signal excited by the laser at the depth z_3 in the Si layer is expressed as follows:

$$\begin{pmatrix} 0 \\ E_{R_{U0}}^{s'(p'),-} \end{pmatrix} = A_{01}^{s'(p')} B(d_1) A_{12}^{s'(p')} B(d_2) A_{23}^{s'(p')} B(z_3) \begin{pmatrix} E_{R_{US}}^{s'(p'),+}(z_3) \\ E_{R_{US}}^{s'(p'),-}(z_3) \end{pmatrix} \tag{11}$$

where $E_{R_{US}}^{s'(p'),-}(z_3)$ is the electric field component of Raman signal source related with 'U' pathway at the depth z_3 in the Si layer and is assumed as 1.

The Raman scattering enhancement factors in this process can be calculated by $F_R^{s'}(z_3) = E_{R_{U0}}^{s',-}$, $F_R^{p'_\perp}(z_3) = E_{R_{U0}}^{p',-}\cos\theta'_3$ and $F_R^{p'_\|}(z_3) = E_{R_{U0}}^{p',-}\sin\theta'_3$. $E_{R_{U0}}^{s'(p'),-}$ can be calculated only by the transfer equation Eq. (11) and $F_R^{s'(p'_\perp,p'_\|)}(z_3)$ can be obtained.

The total Raman intensity of Si peak can be calculated by the formula Eq. (2), when the Raman tensor **R** of the Si peak for Si(100) substrate is considered. Because the penetration depth of laser excitation into Si layer is far less than the actual thickness of Si substrate (d_3), the value of d_{Si} is taken as the penetration depth of laser excitation into Si layer in the numerical integration.

3. Raman intensity of the Si mode, I(Si_0)

I(Si_0) can be calculated directly based on the above model once the thickness of graphene flakes is set to zero.

References

[1] Y. Y. Wang, Z. H. Ni, Z. X. Shen, H. M. Wang and Y. H. Wu, Appl. Phys. Lett., 2008, 92, 043121.

[2] D. Yoon, H. Moon, Y.-W. Son, J. S. Choi, B. H. Park, Y. H. Cha, Y. D. Kim and H. Cheong, Phys. Rev. B, 2009, 80, 125422.

[3] Y. K. Koh, M.-H. Bae, D. G. Cahill, E. Pop, ACS Nano, 2011, 5, 269.

[4] S.-L. Li, H. Miyazaki, H. Song, H. Kuramochi, S. Nakaharai and K. Tsukagoshi, ACS Nano, 2012, 6, 7381.

[5] C. Casiraghi, A. Hartschuh, E. Lidorikis, H. Qian, H. Harutyunyan, T. Gokus, K. S. Novoselov, A. C. Ferrari, Nano Letters, 2007, 7, 2711.

[6] W. P. Han, Y. M. Shi, X. L. Li, S. Q. Luo, Y. Lu and P. H. Tan, Acta Phys. Sin., 2013, 62, 110702.

[7] V. G. Kravets, A. N. Grigorenko, R. R. Nair, P. Blake, S. Anissimova, K. S. Novoselov, A. K. Geim, Phys. Rev. B, 2010, 81, 155413.